Anal. Chem. **2006,** *78,* 2001−2008

Carbohydrate−Protein Interactions by "Clicked" Carbohydrate Self-Assembled Monolayers

Yun Zhang,[†] Sanzhong Luo,[†,‡] Yijun Tang,[§] Lei Yu,[§] Kuang-Yu Hou,[§] Jin-Pei Cheng,[‡] Xiangqun Zeng,*[,§] and Peng George Wang*[,†]

Department of Biochemistry and Chemistry, The Ohio State University, Columbus, Ohio 43210, Department of Chemistry, Oakland University, Rochester, Michigan 48309, and Center for Molecular Science, Institute of Chemistry, Chinese Academy of Sciences, Beijing 100080, China

A Huisgen 1,3-dipolar cycloaddition "click chemistry" was employed to immobilize azido sugars (mannose, lactose, α-Gal) to fabricate carbohydrate self-assembled monolayers (SAMs) on gold. This fabrication was based on preformed SAM templates incorporated with alkyne terminal groups, which could further anchor the azido sugars to form well-packed, stable, and rigid sugar SAMs. The clicked mannose, lactose, and α-Gal trisaccharide SAMs were used in the analysis of specific carbohydrate−protein interactions (i.e., mannose−Con A; ECL−lactose, α-Gal−anti-Gal). The apparent affinity constant of Con A binding to mannose was $(8.7 \pm 2.8) \times 10^5$ and $(3.9 \pm 0.2) \times 10^6$ M^{-1} measured by QCM and SPR, respectively. The apparent affinity constants of lactose binding with ECL and α-Gal binding with polyclonal anti-Gal antibody were determined to be $(4.6 \pm 2.4) \times 10^6$ and $(6.7 \pm 3.3) \times 10^6$ M^{-1}, respectively by QCM. SPR, QCM, AFM, and electrochemistry studies confirmed that the carbohydrate SAM sensors maintained the specificity to their corresponding lectins and nonspecific adsorption on the clicked carbohydrate surface was negligible. This study showed that the clicked carbohydrate SAMs in concert with nonlabel QCM or SPR offered a potent platform for high-throughput characterization of carbohydrate−protein interactions. Such a combination should complement other methods such as ITC and ELISA in a favorable manner and provide insightful knowledge for the corresponding complex glycobiological processes.

Carbohydrate−protein interactions occur through glycoproteins, glycolipids, or polysaccharides displayed on the cell surface with lectins. The binding between lectin and monovalent carbohydrate is typically weak as lectins generally possess shallow binding pockets that are solvent exposed.[1] The studies of protein−carbohydrate interactions have been challenged by the complexity and heterogeneity of cell surfaces, the inherent structure complexity of carbohydrates, and the typically weak affinities of the binding. In the biological context, this limitation has been overcome by multivalent interactions, i.e., simultaneous contact between the clustered carbohydrates on cell surface and protein receptors that contain multiple carbohydrate recognition domains (CRDs).[2]

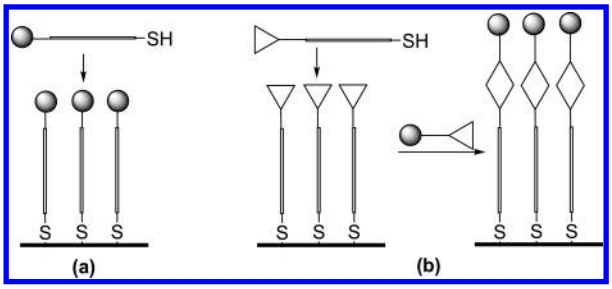

Figure 1. Carbohydrate SAM fabrication strategies on the gold substrate: (a) direct coupling through thiol anchor; (b) indirect coupling through click reactions on preformed template.

The identification of a proper multivalent carbohydrate scaffold has become the prerequisite to the characterization of carbohydrate−protein interactions.[3] Over the past 10 years, a plethora of sugar scaffolds has been explored for studying the protein−carbohydrate interactions (Figure 1).[4] At the same time, the field has seen growing interest in the development of glycoarray technology, i.e., displaying carbohydrates on the surface, which aims at mapping the carbohydrate−protein interactions in a high-throughput manner.[5] The main disadvantage of most of the current glycoarrays is that little has been learned about the nature of the interactions. The self-assembled monolayer (SAM) scaffold has recently appeared as one of the most promising model systems for systematic mechanistic study of the

* To whom correspondence should be addressed. E-mail: pgwang@chemistry.ohio-state.edu; Zeng@oakland.edu.

† The Ohio State University.

‡ Chinese Academy of Sciences.

§ Oakland University.

(1) (a) Kogelberg, H.; Solis, D.; Jimenez−Barbero, J. *Curr. Opin. Struct. Biol.* **2003**, *13*, 646. (b) Gilbert, H. J.; Bolam, D. N.; Szabo, L.; Xie, H.; Williamson, M. P.; Simpson, P. J.; Jamal, S.; Boraston, A. B.; Kilburn, D. G.; Warren, R. A. J. *Spec. Publ.−R. Soc. Chem.* **2002**, *275*, 89. (c) Sharon, N.; Lis, H. *Adv. Exp. Med. Biol.* **2001**, *491*, 1.

(2) Boggs, J. M.; Wang, H.; Gao, W.; Arvanitis, D. N.; Gong, Y.; Min, W. *Glycoconjugate J.* **2004**, *21*, 97.

(3) Kiessling, L. L.; Strong, L. E.; Gestwicki, J. E. *Annu. Rep. Med. Chem.* **2000**, *35*, 321.

(4) (a) Lindhorst, T. K. *Top. Curr. Chem.* **2002**, *218*, 201. (b) Houseman, B. T.; Mrksich, M. *Top. Curr. Chem.* **2002**, *218*, 1. (c) Cloninger, M. J. *Curr. Opin. Chem. Biol.* **2002**, *6*, 742. (d) Kiessling, L. L.; Gestwicki, J. E.; Strong, L. E. *Curr. Opin. Chem. Biol.* **2000**, *4*, 696.

(5) (a) Feizi, T.; Fazio, F.; Chai, W.; Wong, C. H. *Curr. Opin. Struct. Biol.* **2003**, *13*, 637. (b) Disney, M. D.; Seeberger, P. H. *Drug Discovery Today: Targets* **2004**, *3*, 151.

10.1021/ac051919+ CCC: $33.50
Published on Web 01/28/2006

multivalent interaction.[6] Carbohydrate SAMs offer extensive control over the ligands presenting pattern, density, and orientation, which are beneficial to elicit a clear structure−activity relationship of these multivalent interactions. More importantly, SAMs have been well applied to surface-based real-time, label-free analysis methods such as surface plasmon resonance (SPR) and quartz crystal microbalance (QCM). The combination of SAM and SPR has been quite effective in elucidating the binding pattern, affinity (either weak or strong), and specificity of lectins.

Among several classes of SAMs,[7] self-assembled monolayers of alkanethiolates on gold currently hold the best model system[8] since these monolayers form spontaneously by adsorption of alkanethiols from their solutions onto clean gold surfaces. Two general strategies have been used for making sugar SAMs on gold. The first is based on the separate synthesis of the sugar derivatives with a pendant alkanethiol group and subsequent formation of SAMs (Figure 1a). The drawback of this strategy comes from the tremendous synthetic effort for sugars anchored with a pendant alkanethiol. Furthermore, as the complexity of tethered sugars increases, there is no guarantee that the molecules will pack to form a structurally well-defined monolayer.[4b]

The second strategy is based on the direct chemical transformation of the functionalized SAMs (Figure 1b). This method introduces sugar moieties onto the preformed functionalized SAMs using selected chemical reactions.[9] Obviously, the identification of a good reaction is the critical determinant for fabrication of sugar SAMs. Previously, several interphase reactions have been identified for anchoring sugar units, including Diels−Alder reaction,[10] thiol addition to activated maleimide,[11] and disulfide exchange.[12] Here we describe using a "click chemistry" method to fabricate sugar SAMs on gold substrate. By defining click, the reaction should tolerate a variety of conditions and functionalities and occur quantitatively with high fidelity. Those requirements are characteristic of click chemistry, as defined by Sharpless.[13] Since the properties of the monolayer depend on the terminal functional group of the precursor alkanethiol, virtually any surface can be prepared using well-developed click chemistry.

Among identified click reactions, i.e., cycloaddition, ring opening to nonaldol type carbonyl chemistry, and oxidation addition,[14] the Cu(I)-catalyzed heterocycloaddition of terminal azide to terminal alkyne has recently gained more interest since this click reaction may take place in aqueous media.[15] This reaction also tolerates a variety of conditions and functionalities and occurs quantitatively with high fidelity. The literature shows that this reaction has been applied successfully in the capture of saccharides bound noncovalently or covalently onto microtiter plates.[16] Collman and co-workers made azide-terminated SAMs on a gold surface and attached oligodeoxyribonucleotide with reactive acetylene groups to the SAMs.[17] The result was a well-defined structure of an oligonucleotide probe. Wong et al. also used this click reaction to make oligosaccharide arrays for the screening of complex carbohydrates.[18] Consequently, we explored in this report Cu(I)-catalyzed Huisgen 1, 3-dipolar cycloaddition reaction, as a general strategy for fabricating sugar-SAMs. In particular, we designed an activated alkyne linker on the gold surface that could be readily coupled with azido sugars through Cu(I)-catalyzed Huisgen 1,3-dipolar cycloaddition reaction. This cycloaddition system is best for glycoarray fabrication since azido sugars are readily accessible and have been used extensively in understanding cellular processes through chemoselective ligation reaction between an azide and a functionalized phosphine, termed the Staudinger ligation by Bertozzi and others.[19] This strategy significantly reduces the synthetic labor for carbohydrate thiolates and promises rapid and flexible construction of arrays of carbohydrate SAMs for elucidating carbohydrate functions in biological systems.[20−22] The specificity of these carbohydrate SAMs and the generality of this reaction were studied by analyzing the specific binding of proteins to mannose (monosaccharide), lactose (disaccharide), and α-Gal (trisaccharide) SAMs.

EXPERIMENTAL SECTION

Chemicals and Materials. Reagents were obtained from commercial suppliers and used without further purification. All glassware and syringes were dried in an oven overnight, allowed to cool, and stored under a positive pressure of argon before use. Dichloromethane was distilled and dried with CaH_2. Compounds were purified by flash chromatography (FC) on silica gel. Thin-layer chromatography was run on SiO_2 60F254 (Merck) and visualized with UV, H_2SO_4, and $KMnO_4$ reagents. ^1H (250 and 500 MHz) and ^{13}C (62.5 and 125 MHz) NMR spectra were measured using Bruker NMR instrument. Concanavalin A (Con A) and *Erythrina cristagalli* lectins (ECLs) were purchased from Sigma. Anti-Gal antibody was purified by α-Gal affinity column from human blood serum. All remaining materials for biological assays were purchased from Sigma.

***N,N′*-(Dithiodidecane-10,1-diyl)bispropiolamide (NDDA).** To a solution of 10,10′-dithiobisdecan-1-amine (0.9 g, 2.39 mmol) and propiolic acid (0.4 g, 5.74 mmol) in dichloromethane (30 mL), dicyclohexylcarbodiimide (1.3 g, 6.31 mmol) was added portion-

(6) (a) Schreiber, F. *J. Phys.: Condens. Matter* **2004**, *16*, R881. (b) Chaki, N. K.; Vijayamohanan, K. *Biosens. Bioelectron.* **2002**, *17*, 1.
(7) (a) Mann, D. A.; Kanai, M.; Maly, D. J. Kiessling, L. L. *J. Am. Chem. Soc.* **1998**, *120*, 10575. (b) Vogel, J.; Bendas, G.; Bakowsky, U.; Hummel, G.; Schmidt, R. R.; Kettmann, U.; Rothe, U. *Biochim. Biophys. Acta* **1998**, *1372*, 205.
(8) (a) Gooding, J. J.; Mearns, F.; Yang, W.; Liu, J. *Electroanalysis* **2003**, *15*, 81. (b) Mrksich, M. *Chem. Soc. Rev.* **2000**, *29*, 267. (c) Mrksich, M. *Curr. Opin. Chem. Biol.* **2002**, *6*, 794.
(9) (a) Sullivan, T. P.; Huck, W. T. S. *Eur. J. Org. Chem.* **2003**, 17. (b) Flink, S.; van Veggel, F. C. J. M.; Reinhoudt, D. N. *Adv. Mater.* **2000**, *12*, 1315.
(10) Houseman, B. T.; Mrksich, M. *Chem. Biol.* **2002**, *9*, 443.
(11) Houseman, B. T.; Gawalt, E. S.; Mrksich, M. *Langmuir* **2003**, *19*, 1522.
(12) Smith, E. A.; Thomas, W. D.; Kiessling, L. L.; Corn, R. M. *J. Am. Chem. Soc.* **2003**, *125*, 6140.
(13) Kolb, H. C. Finn, M. G.; Sharpless, K. B. *Angew. Chem., Int. Ed.* **2001**, *40*, 2004.
(14) Kolb, H. C.; Sharpless, K. B. *Drug Discovery Today* **2003**, *8*, 1128−1137.
(15) Rostovtsev, V. V.; Green, L. G.; Fokin, V. V.; Sharpless, K. B. *Angew. Chem., Int. Ed.* **2002**, *41*, 2596−2599.
(16) (a) Bryan, M. C.; Fazio, F.; Lee, H. K.; Huang, C. Y.; Chang, A.; Best, M. D.; Calarese, D. A.; Blixt, O.; Paulson, J. C.; Burton, D. *J. Am. Chem. Soc.* **2004**, *126*, 8640. (b) Fazio, F.; Bryan, M. C.; Blixt, O.; Paulson, J. C.; Wong, C.-H. *J. Am. Chem. Soc.* **2002**, *124*, 14397.
(17) Devaraj, N. K.; Miller, G. P.; Ebina, W.; Kakaradov, B.; Collman, J. P.; Kool, E. T.; Chidsey, C. E. D. *J. Am. Chem. Soc.* **2005**, *127*, 8600−8601.
(18) Bryan, M. C.; Fazio, F.; Lee, H.-K.; Huang, C.-Y.; Chang, A.; Best, M. D.; Calarese, D. A.; Blix, O.; Paulson, J. C.; Burton, D.; Wilson, I. A.; Wong, C.-H. *J. Am. Chem. Soc.* **2004**, *126*, 8640−8641.
(19) Saxon, E.; Bertozzi, C. R. *Science* **2000**, *287*, 2007.
(20) Ratner, D. M.; Adams, E. W.; Disney, M. D.; Seeberger, P. H. *ChemBioChem* **2004**, *5*, 1375−1383.
(21) Disney, M. D.; Seeberger, P. H. *Drug Discovery Today: Targets* **2004**, *3*, 151−158.
(22) Feizi, T.; Fazio, F.; Chai, W.; Wong, C.-H. *Curr. Opin. Struct. Biol.* **2003**, *13*, 637−645.

wise at 0 °C. The resultant mixture was stirred at 0 °C for 1 h and stirred at room temperature for another 1 h. The mixture was filtered to remove the insoluble byproducts and the filtered solution was concentrated under vacuum. The residue was purified by FC on silica gel (hexane/ethyl acetate, 2/1 → 1/2) to afford the desired product as white powder (0.7 g, 61%). ^{1}H NMR (250 MHz): δ 1.28 (24H, s, br), 1.49−1.55 (4H, m), 1.63−1.69 (4H, m), 2.67 (4H, t, J = 7.2 Hz), 2.76 (2H, s), 2.73 (4H, t, J = 6.2 Hz), 5.97 (2H, s br). ^{13}C NMR (62.5 MHz): δ 26.8, 28.9, 29.6, 29.8, 39.6, 40.3, 73.3, 77.6, 152.5. HRMS for $C_{26}H_{44}N_2O_2S_2Na$ (M + Na), calcd, 503.2736; found, 503.2714.

Azido Sugars. A mixture of trichloroacetimidate donor[23] (1.0 equiv), azidotriethylene glycol acceptor (2.0 equiv), and molecular sieves (4Å powder, 100 mg/mmol) in CH_2Cl_2 was stirred at room temperature for 30 min. The mixture was then cooled to −60 °C, and a solution of TMSOTf (20 mol %) in CH_2Cl_2 was added. The stirring was kept at −60 °C for 1 h, and then the resulting mixture was allowed to warm to room temperature and stirred for an additional 2 h. Following the typical workup procedure, the obtained residue was purified by FC on silica gel to afford the desired peracetylated products. Subsequent treatment with MeONa in methanol (1 mM) for 2 h at room temperature and neutralization with Amberlite 120 forwarded the desired azido sugars.

Azidomannose. Colorless syrup, 71% yield for two steps. ^{1}H NMR (500 MHz): δ 3.40 (2H, t), 3.60 (3H, m), 3.66−3.75 (12H, m), 3.78−3.88 (4H, m), 3.98 (1H, m), 4.85 (1H, d, J = 2.0 Hz). ^{13}C NMR (125 MHz): δ 50.2, 60.9, 66.4, 66.8, 69.3, 69.5, 69.6, 69.7, 70.0, 70.5, 72.7, 100.0. HRMS for $C_{12}H_{23}N_3O_8Na$ (M + Na), calcd, 360.1377; found, 360.1359.

Azidolactose. Colorless syrup, 70% yield for two steps. ^{1}H NMR (500 MHz): δ 3.47 (2H, t, J = 5 Hz), 3.50−3.56 (2H, m), 3.61−3.64 (4H, m), 3.68−3.76 (14H, m), 3.78−3.83 (4H, m), 3.88 (1H, d, J = 3.5 Hz), 3.93 (1H, dd, J = 2.0 and 12 Hz), 4.02−4.04 (1H, m), 4.42 (1H, d, J = 8.0 Hz), 4.48 (1H, d, J = 8.0 Hz). ^{13}C NMR (125 MHz): δ 50.2, 60.1, 61.0, 68.6, 68.8, 69.2, 69.5, 69.6, 69.7, 71.0, 72.6, 72.8, 74.3, 74.8, 75.4, 78.4, 102.1, 103.0. HRMS for $C_{18}H_{33}N_3O_{13}Na$ (M + Na), calcd, 522.1905; found, 522.1908.

Azido-α-Gal. Colorless syrup, 58% yield for two steps. ^{1}H NMR (500 MHz): δ 3.47 (2H, t, J = 5 Hz), 3.56−3.58 (1H, m), 3.60−3.65 (5H, m), 3.69−3.84 (25 H, m), 3.90−4.04 (4H, m), 4.14−4.17 (2H, m), 4.48 (1H, d, J = 8.0 Hz), 4.49 (1H, d, J = 8.0 Hz), 5.10 (1H, d, J = 4.0 Hz). ^{13}C NMR (125 MHz): δ 50.2, 60.4, 60.9, 61.0, 64.8, 68.2, 68.8, 69.1, 69.2, 69.3, 69.5, 69.6, 69.7, 70.8, 71.7, 72.8, 74.4, 74.8, 75.1, 77.2, 78.7, 95.5, 102.1, 102.9. HRMS for $C_{24}H_{43}N_3O_{18}Na$ (M + Na), calcd, 684.2434; found, 684.2424.

Quartz Crystal Microbalance. The nonpolished gold quartz crystal (International Crystal Manufacturing Co. Inc.) was mounted in a custom-made Kel-F cell. It was cleaned three times using concentrated nitric acid and sulfuric acid (1:1 v/v), biograde water (i.e., resistance greater than 18 MΩ and further radiated by UV light and filtered with a 0.2-μm filter), and ethanol in series, and then the cell was dried using a nitrogen stream. The frequency of the electrode was measured both dry and in PBS, pH 7.2. One side of the gold quartz crystal was incubated in a solution of 0.10 mM NDDA disulfide in anhydrous ethanol at 4 °C overnight. After incubation, the gold surface was washed with ethanol and biograde water and dried under nitrogen to afford NDDA SAM. To click the sugar onto the SAM NDDA, the preformed NDDA SAM template was incubated in a solution of 0.1 M azido sugars (i.e., azidomannose, azidolactose, or azido-α-Gal) in clicking buffer (EtOH:H_2O = 1:1, v/v; $CuSO_4$ 1 mM, sodium ascorbate 5 mM) at room temperature for 10 h. After incubation, the gold surface was washed with ethanol and biograde water and dried under nitrogen. Any unoccupied clicking sites on the surface were then blocked by incubation with 0.1 M azidotris(ethylene oxide) glycol in the clicking buffer for another 10 h. Subsequent washing and drying afforded a blocked sugar SAM, which was subsequently used for the binding assay by adding various concentrations of lectin in aliquots with stirring to the QCM cell. The change in frequency and damping resistance of the QCM were monitored simultaneously using a network/spectrum/impedance analyzer (Agilent 4395A) controlled by a PC via an Intel card.

Electrochemical Characterization. The gold electrode of the QCM with immobilized SAM was used as the working electrode. A platinum wire and a saturated calomel electrode were used as counter and reference electrodes, respectively. Cyclic voltammetry and electrochemical impedance spectroscopy were carried out in a solution of 0.1 M $NaClO_4$ containing 1 mM $K_3Fe(CN)_6$/$K_4Fe(CN)_6$ using a Parstat 2263 advanced electrochemical system (Princeton Applied Research).

Surface Plasmon Resonance. A new Biacore gold chip was immersed in 0.1 mM NDDA solution for 4 h. The sample flow cell (FC2) was incubated with a mixture of 14 μM azidomannose, 1 mM $CuSO_4$, and 1 mM sodium ascorbate for 8 h. Both the reference flow cell (FC1) and sample flow cell were then incubated with 0.1 M azidotris(ethylene oxide) glycol overnight. Azidotris-(ethylene oxide) was used as a blocking reagent to take up any unreacted alkynyl terminals of NDDA. Both FC1 and FC2 were then incubated with 10 mM 2-mercaptoethanol for 4.5 h so that any unoccupied gold sites could be blocked. The constructed sensor chip was then incubated with 0.005% BSA for 30 min. Although the blocking processes do not affect the later sugar−protein binding in our experiments, it was still applied to be consistent with previous work, so that the results can be compared.

Con A solutions with concentrations varying from 0.56 to 9.0 μM (monomer) were injected into the Biacore X SPR instrument and flowed through both FC1 and FC2. All Con A solutions contained 1 mM $CaCl_2$ and 1 mM $MnCl_2$ as the catalyst except the control experiments.

AFM Characterizations. A polished quartz plate coated with a thin layer of gold (~100 nm) over 50 Å of Cr by vapor deposition had a smooth surface and was used as substrate. After clicking azidomannose and azidotriethylene glycol blocker on the NDDA SAM surface (Figure 2), the modified quartz substrate was soaked in a Con A solution containing catalysts Ca^{2+} and Mn^{2+} for 6 h followed by thorough rinsing with water and PBS buffer. AFM images were obtained with a contact mode Molecular Imaging PicoScan Atomic Force Microscope and a MicroMasch (Estonia) ultrasharp (Rc < 10 nm) and ultrasoft (force constant, 0.03 N/m) silicon cantilever. The scan rate was three lines/s, and the resolution was 512 data points/line. Both the cantilever and the sample were in a PBS buffer filled liquid cell during the experiments.

(23) Qiu, D.; Schmidt, R. R. *Liebigs Ann. Chem.* **1992**, *3*, 217.

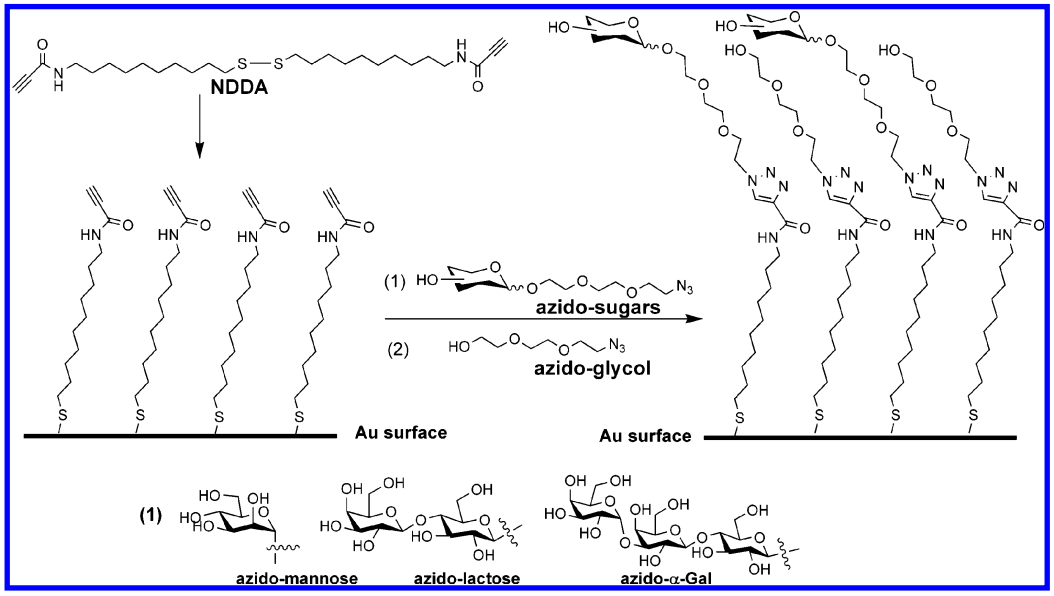

Figure 2. Carbohydrate (i.e., mannose, lactose, or α-Gal) SAM fabricating strategies using a Huisgen 1,3-dipolar cycloaddition "click" chemistry.

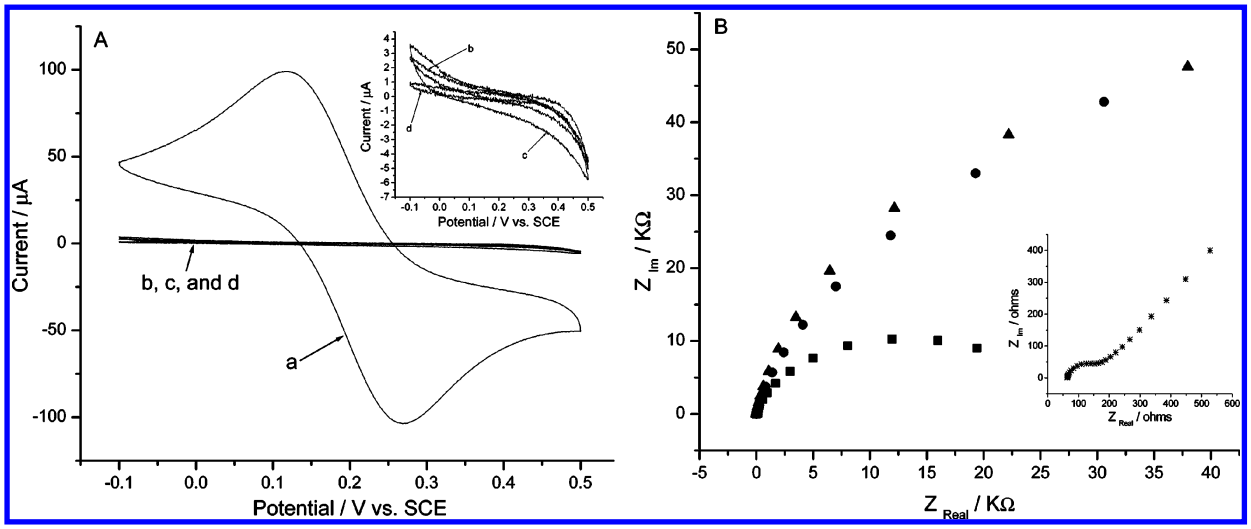

Figure 3. (A) CVs of 1 mM $K_4Fe(CN)_6/K_3Fe(CN)_6$ in 0.1 M $NaClO_4$ on bare gold electrode (a), SAM of NDDA (b), SAM of NDDA + azidomannose (c), and SAM of NDDA + azidomannose + azidoglycol (d) modified electrodes. Scan rate, 50 mV/s. (B) EIS Nyquist plots obtained with bare gold electrode (∗), SAM of NDDA (■), SAM of NDDA + azidomannose (▲), and SAM of NDDA + azidomannose + azidoglycol (●) modified electrodes. Frequency range is 0.1 Hz−100 kHz. Bias potential equals to open circuit potential. AC amplitude is 10 mV.

RESULTS AND DISCUSSIONS

For the successful application of the SAMs, several key factors have been identified, and these include (1) SAM fabrication strategy, (2) ligands presenting density, and (3) surface resistance to nonspecific adsorption. Several structure motifs were incorporated into the preformed SAMs shown in Figure 2. First, a long chain alkyl (C_{10}) disulfide linker NDDA with terminal alkyne group was selected to form the rigid and highly packed monolayer as the template for the fabrication of carbohydrate SAMs. Among various options, an amide linkage was selected to connect the alkyl chain and the alkyne group. This linkage provided an activated alkyne moiety, which was readily coupled to the azido sugars. The incorporated amide group formed hydrogen bonds within the monolayer matrix, increasing the stability and rigidness of the carbohydrate SAM.[24,25] Second, tris(ethylene oxide) glycol was incorporated into the azido sugars to eliminate nonspecific adsorptions.[26] Finally, azidotris(ethylene oxide) glycol was synthesized and used to react with any unreacted alkynyl terminals of NDDA after azido sugar click reaction to further block the nonspecific adsorption.

Electrochemical Characterization of the Saccharide Biosensor. The formation of a rigid mannose SAM was verified by cyclic voltammetry and electrochemical impedance measurements. SAMs of NDDA, azidomannose, and azidotris(ethylene oxide) glycol are electrochemically inert in the potential range studied.

As shown in Figure 3A, CV on the bare gold surface gave reversible redox peaks of $K_4Fe(CN)_6/K_3Fe(CN)_6$. Faradaic current was dramatically attenuated once a SAM of NDDA was formed on the surface. Treatment of the NDDA SAM with azidomannose

(24) Clegg, R. S.; Hutchison, J. E. *J. Am. Chem. Soc.* **1999**, *121*, 5319−5327.

(25) Valiokas, R.; Svedhem, S.; Svensson, S. C. T.; Liedberg B. *Langmuir* **1999**, *15*, 3390−3394.

(26) Prime, K. L.; Whitesides, G. M. *J. Am. Chem. Soc.* **1993**, *115*, 10714−10721.

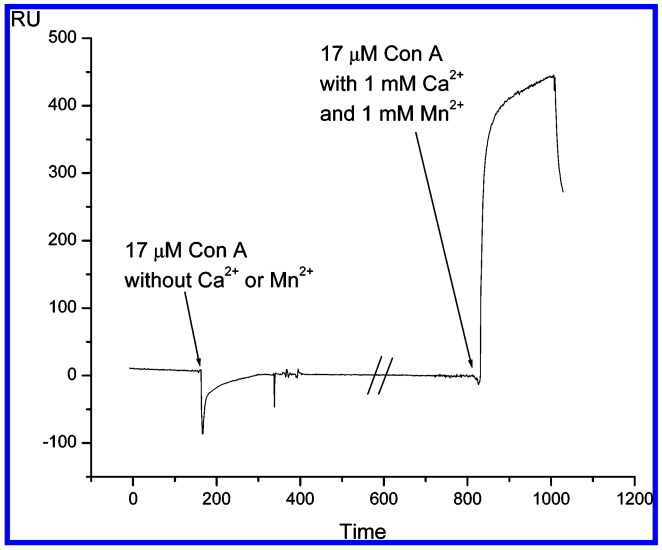

Figure 4. Specific adsorption of Con A on the mannose SAM in the presence of 1 mM Ca^{2+} and Mn^{2+}. The time scale is only a relative representation. The two injections were performed in separate cycles, and the sensograms were put in one figure for comparison.

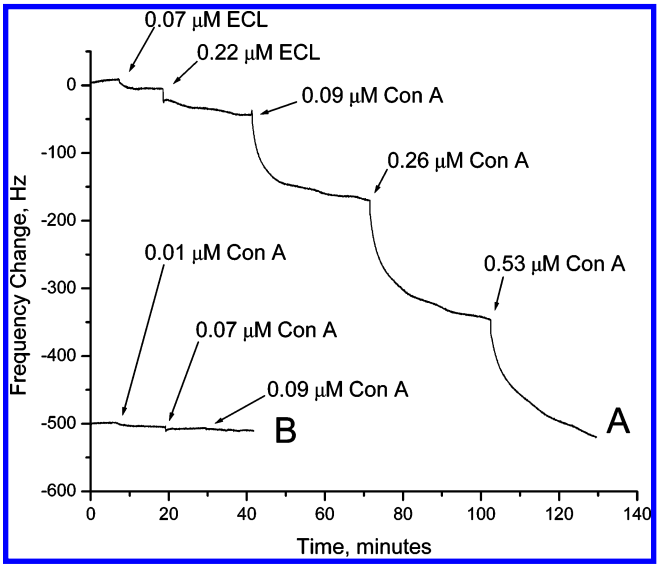

Figure 5. QCM analysis of ECL and Con A binding on (A) mannose SAM and (B) lactose SAM. ECL is specific to lactose but not to mannose, while Con A is specific to mannose but not to lactose.

under clicking conditions, and further clicking with azidotris(ethylene oxide) glycol did not significantly affect the features of the CVs, since the redox reactions on the electrode surface were mostly blocked by the NDDA SAM. However, the minor change of the SAM properties was revealed by corresponding Nyquist plots (Figure 3B). While the electron-transfer resistance(R_{et}) of the $Fe(CN)_6^{IV}/Fe(CN)_6^{III}$ redox reactions increased drastically after the formation of the NDDA SAM. The reaction of NDDA SAM with azidomannose, and the subsequent reaction with azidotris(ethylene oxide) glycol resulted in further increase of R_{et}, suggesting the retention of a highly compact structure at these steps. The change of R_{et} after the clicking of azidotriethylene glycol was not significant, compared to the R_{et} after the click of azidomannose. These experiments supported the existence of highly compact SAM of the azidomannose and azidoglycol on the surface. The highly compact monolayer may result from the highly aligned mannose and the glycol moieties.

Control Experiments. We further characterized the clicking mannose SAM by SPR, QCM and AFM to verify the formation of mannose SAM and its specificity to lectin Con A.

SPR. Con A is one of the most widely used and well-characterized lectins. Con A has broad applicability primarily because it recognizes a commonly occurring sugar structure, α-linked mannose. At neutral and alkaline pH, Con A exists as a tetramer of four identical subunits of ~26 000 Da each. Below pH 5.6, Con A dissociates into active dimmers of 52 000 Da. Con A has an isoelectric point of pH ~5 and requires calcium or manganese ions at each of its four saccharide binding sites. Therefore, the Con A solution without the catalytic ions was analyzed for nonspecific adsorption of Con A. SPR experiment showed that Con A did not bind with mannose unless Ca^{2+} and Mn^{2+} were present. Injection 1 was 17 μM Con A solution, and injection 2 was the same concentration of Con A solution containing 1 mM Ca^{2+} and 1 mM Mn^{2+} (Figure 4).

QCM. ECL is a 54 000 Da glycoprotein consisting of two different subunits of approximately 28 000 and 26 000 Da. It has specificity toward galactose residues and appears to have the highest binding activity toward galactosyl (β-1,4) *N*-acetylglucosamine. Shown in Figure 5, addition of ECL generated a frequency change of ~40 Hz at the concentration of 0.22 μM, while Con A of the similar concentration (0.26 μM) generated a frequency change of ~170 Hz, four times larger than ECL. Even a smaller concentration of Con A (0.09 μM) could generate a large frequency change of over 120 Hz on the same chip. This study demonstrated that the mannose SAM retained its specificity to Con A, but it has slight cross activity with ECL. Curve B of Figure 5 indicates that there was little cross activity of Con A with lactose; that is, nonspecific adsorption of Con A on lactose SAM was negligible with a frequency change of ~10 Hz at the concentration of 0.09 μM. Figure 7 further demonstrates that mannose SAM responded sensitively and specifically to the addition of Con A and it had little nonspecific adsorption with BSA.

AFM. Panels A and B in Figure 6 are the AFM images of the mannose SAM prepared identically using the above click chemistry strategy shown in Figure 2 before and after the binding with Con A. Little change was observed after the formation of mannose SAM (Figure 6A), compared to the bare substrate (data not shown). After the incubation of mannose SAM in the Con A solution, the roughness of the surface changed drastically, Figure 6B. The change of the roughness was also echoed in the significant increase of the data diversity shown in the image histograms (Figure 6C, D). The average *Z* dimension values increased from ~2.5 nm to ~4.0 nm. The maximum peak-to-valley distance was ~6 nm and the average value was ~4 nm (Figure 6D). The average height of 4−6 nm was smaller than the physical size of Con A obtained by the X-ray crystallographic method and tapping mode AFM (~6.3−8.9 nm).[27,28] The smaller value in our case was probably due to the tip-induced changes when contact mode was used. The average full width at half-maximum was ~50−80 nm, which was in agreement with AFM image of Con A

(27) Lebed, K.; Pyka-Fosciak, G.; Raczkowska, J.; Lekka, M.; Styczen, J. *J. Phys.: Condens. Matter* **2005**, *17*, S1447−S1458.
(28) Yonzon, C. R.; Jeoung, E.; Zou, S. L.; Schatz, G. C.; Mrksich, M.; Van Duyne, R. P. *J. Am. Chem. Soc.* **2004**, *126*, 12699−12676.

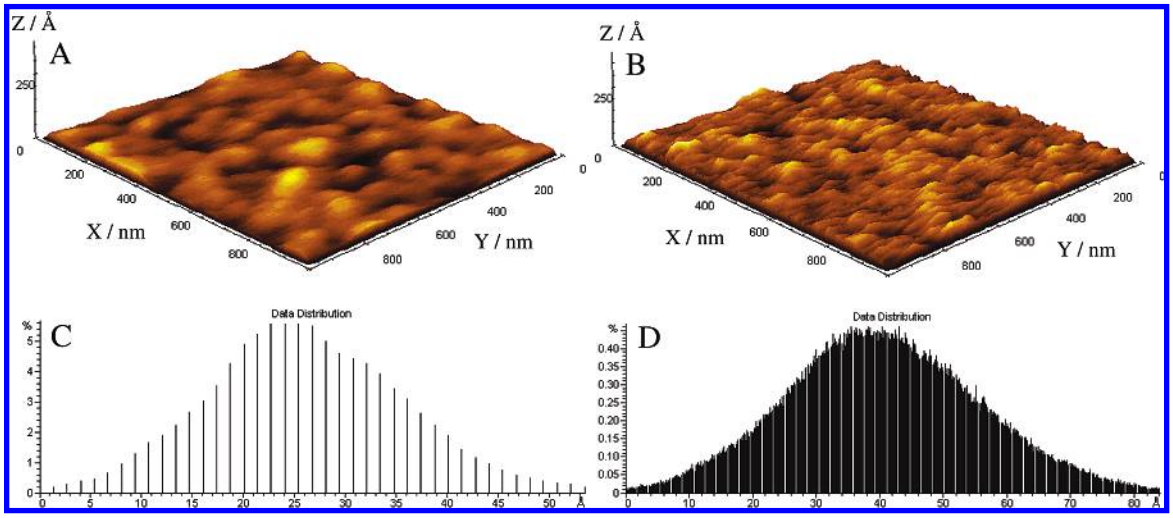

Figure 6. 1 μm × 1 μm × 250 Å AFM 3D topography images of the SAM of NDDA + azidomannose + azidoglycol before (A) and after (B) it was soaked in Con A solution for 6 h. Histograms of the data distribution in *Z* dimension before (C) and after (D) the binding of ConA.

reported (~65 nm).[27] The larger observed value than its real dimension was rationalized as a result of the tip convolution effect. The images did not change after multiple scans, indicating a strong binding of Con A on the surface. The defects or pinholes of the SAM could not be resolved at our experimental condition.

Since the polished gold quartz crystal substrates used in the AFM study are not atomically flat, it is difficult to resolve individual Con A molecules in the images. However, the consistent change of the roughness occurred in the full range of the image in Figure 6B indicates an even distribution of the Con A molecules on the surface of the substrate, thus a relatively high coverage of mannose on the gold surface. SPR study showed the maximum amount of Con A bound on the mannose surface was ~2.0×10^{-13} mol/cm^2. Assuming the one-to-one binding of ConA and mannose, the minimum coverage of mannose should be 2.0×10^{-13} mol/cm^2. Even though QCM could provide additional information of mannose and Con A surface coverage by measuring the dry frequency of gold quartz crystal at each SAM formation step, it was difficult to reproduce the washing and drying to be identical at each step so that, in the current study, we were unable to provide the absolute surface coverage of mannose SAM.

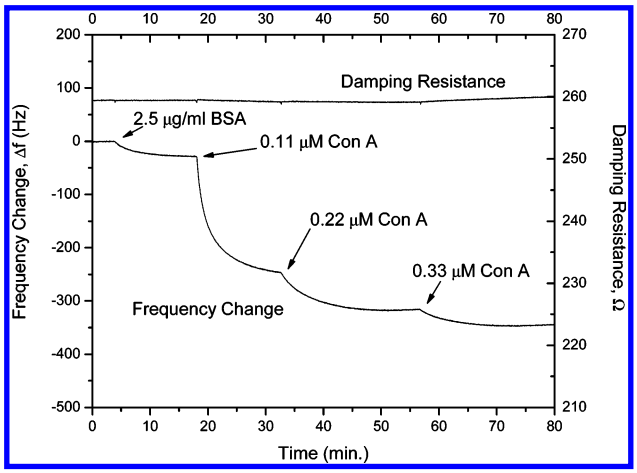

Figure 7. Frequency change vs time and damping resistance vs time curves for immobilized mannose SAM in the presence of BSA and various concentrations of ConA.

Binding Analysis. During the binding analysis, the rigidity of the mannose monolayer was evaluated by measuring the damping resistance determined by fitting the impedance spectra of the resonator with the Butterworth−Van Dyek equivalent circuit. This analysis could assess the validity of the Sauerbrey equation for QCM quantification of biomolecular interactions. The change of damping resistance was $|\Delta R_q|/R_q \leq 0.2\%$ (Figure 7), indicating that the monolayer was exhibiting rigid, rather than viscoelastic behavior in the binding process and the mannose SAMs were well-applied to QCM analysis.

The binding of three common sugar epitopes with lectin and protein (i.e., mannose−Con A, lactose−ECL, α-Gal−anti-Gal) was studied and analyzed with the Langmuir adsorption model. All three carbohydrates were immobilized through the above click chemistry. The frequency change at equilibrium was related to the lectin/protein concentration according to the following equation.[29]

$$\frac{C}{\Delta f} = \frac{C}{\Delta f_{max}} + \frac{1}{\Delta f_{max}} \cdot \frac{1}{K_A} \quad (1)$$

where Δf is the frequency decrease at equilibrium, C is the lectin concentration, Δf_{max} is the frequency change when C is infinity, and K_A is the apparent binding affinity. The plot according to the eq 1 generated a straight line and the ratio of slope to intercept was K_A.

Similar to eq 1, the following equation was used for the SPR analysis.

$$\frac{1}{R_{eq}} = \frac{1}{R_{max} K_A} \cdot \frac{1}{C} + \frac{1}{R_{max}} \quad (2)$$

where R_{eq} is the SPR response to the injection of lectin with

(29) (a) Ebara, Y.; Itakura, K.; Okahata, Y. *Langmuir* **1996**, *12*, 5165−5170. (b) Okahata, Y.; Natsuura, K.; Ito, K.; Ebara, Y. *Langmuir* **1996**, *12*, 1023−1026. (c) Yang, M.; Yau, H. C. M.; Chan, H. L. *Langmuir* **1998**, *14*, 6121−6129.

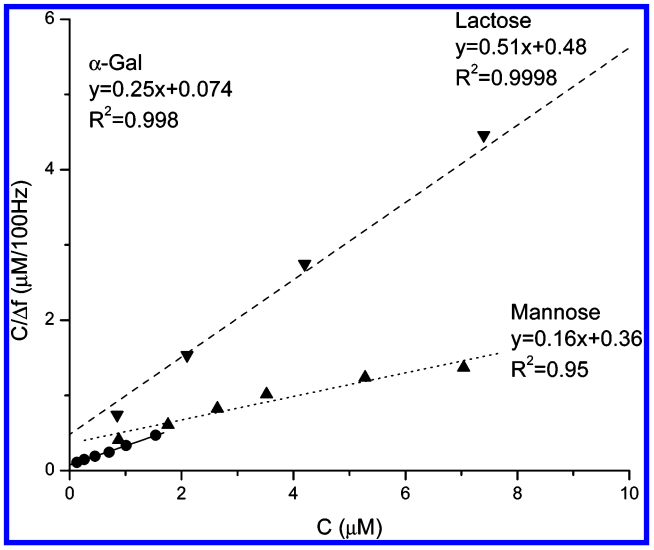

Figure 8. Langmuir isotherm plots for (▲) Con A binding with mannose SAM, (▼) ECL binding with lactose SAM, and (●) anti α-Gal binding with α-Gal SAM by QCM study.

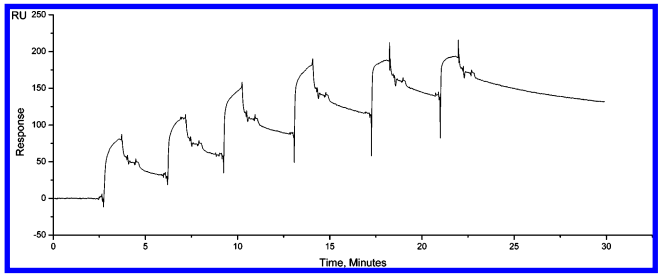

Figure 9. SPR sensorgram of Con A binding to mannose sensor chip. The concentrations of Con A injected were 0.56, 1.12, 2.25, 4.5, 9.0, and 9.0 μM (monomer). All the injection contained 1 mM Ca^{2+} and 1 mM Mn^{2+}.

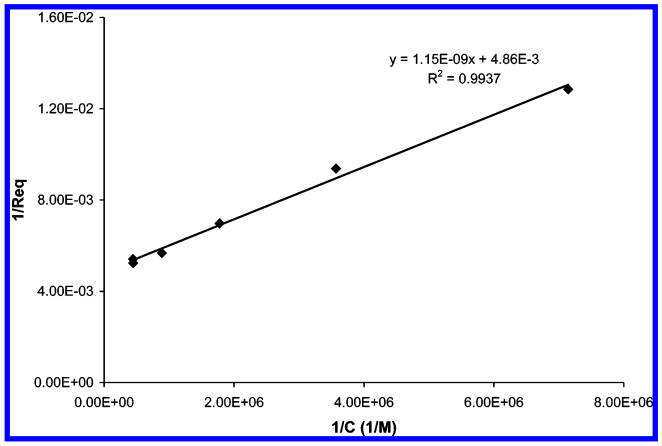

Figure 10. $1/R_{eq}$ vs $1/C$ plot by SPR. The apparent affinity constant generated from this straight line was 4.2×10^6 M^{-1} for Con A.

concentration of C at equilibrium and R_{max} is the equilibrium response when C is infinity.

The value of K_A for Con A binding with mannose was determined to be $(8.7 \pm 2.8) \times 10^5$ M^{-1} ($n = 5$) by QCM technique (Figure 8) and $(3.9 \pm 0.2) \times 10^6$ M^{-1} ($n = 3$) by SPR technique (Figure 9 and Figure 10). The apparent affinity constants were determined to be $(4.6 \pm 2.4) \times 10^6$ M^{-1} ($n = 5$) for lactose binding with ECL and $(6.7 \pm 3.3) \times 10^6$ M^{-1} ($n = 2$) for α-Gal binding with polyclonal anti-Gal by QCM technique (Figure 8).

For the SPR analysis, we have developed a nonregeneration kinetic and thermodynamic analysis protocol (Figure 9) in which there was no regeneration between consecutive injections.[30] Using the nonregeneration protocol, R_{eq} for each injection could be obtained, which was plotted in Figure 10 accordingly.

For mannose−Con A binding, our SPR study was in close agreement with the Smith et al.[12] SPR study (i.e., K_A value of $(5.6 \pm 1.7) \times 10^6$ M^{-1}). In their study, mannose was modified with a disulfide to form gold mannose SAM. Their strategy required tremendous synthetic effort compared to the click SAM strategy that we used in this report. The slightly higher value of SPR results compared to those of the QCM study was rationalized by the avidity effect (i.e., the number of binding sites affected the binding constant). The SPR gold chip used in our study was optically flat and smoother than that of nonpolished gold quartz crystals. A better SAM was formed on the SPR gold chip, and higher avidity was observed on the SPR gold surface. Similarly, for α-Gal binding with polyclonal anti-Gal, the clicked α-Gal SAM gave a 4-fold smaller affinity constant than our earlier QCM study[31] (6.7×10^6 vs 2.8×10^7). In the early study, the α-Gal was modified with a thiol group; consequently, higher density of α-Gal was immobilized than our current click chemistry strategies. The avidity effect also leads to significant enhancement of affinity for azidolactose (~1000-fold)[32] as well as that for azidomannose (>100 fold)[33] compared to the solution-phase assay by ITC study.

CONCLUSIONS

We present here a robust and versatile strategy for fabricating carbohydrate self-assembled monolayers by taking advantage of the recent availability of complex carbohydrate materials from chemoenzymatic syntheses and the inherent quick, clean, high-fidelity characters of click chemistry. The monolayer is structurally well defined and offers wide synthetic flexibility in tailoring with different saccharides, which facilitates the use of QCM and SPR as highly effective nonlabeled sensors. These sensors not only can be used to obtain information on the kinetics and thermodynamics data of the lectin−sugar recognition in hormone receptor studies, mitogenic assays, characterization of normal and malignant cells, glycoprotein purification, viral antigen isolation, dextran and mannan fractionation, cell agglutination studies, bacterial aggregation, membrane fluidity and lateral mobility investigations, turbidimetric assays for sugars, and lymphokine production , but also can be used to understand the underlying forces that govern these interactions. Both SPR and QCM are nonlabeled biosensors, which are free from the time- and cost-demanding labeling step and, subsequently, eliminate any possible interference in the "true" binding process due to the presence of the labels. As such, this method allows the analysis of real-time interactions and is able to deliver high-quality, detailed information content for carbohydrate−protein interactions. The applications of click SAM methods for the immobilization of other sugars and studying of their binding

(30) Tang, Y; Mernaugh, R.; Zeng, X. *Anal. Chem.* In press (ac051868g).
(31) Zhang, Y.; Telyatnikov, V.; Sathe, M.; Zeng, X.; Wang, P. G. *J. Am. Chem. Soc.* **2003**, *125*, 9292−9293.
(32) Svensson, C.; Teneberg, S.; Nilsson, C. L.; Kjellberg, A.; Schwarz, F. P.; Sharon, N.; Krengel, U. *J. Mol. Biol.* **2002**, *321*, 69−83.
(33) Mandal, D. K.; Kishore, N.; Brewer, C. F. *Biochemistry* **1994**, *33*, 1149−1156.

with protein interactions by SPR and QCM are ongoing in our laboratory.

ACKNOWLEDGMENT

P.G.W. acknowledges support from The Ohio State University Ohio Eminent Scholar adornments. X.Z. thanks Oakland University and the NIH (4R33 EB000672-02) for support. S.L. and J.-P.C. thank the National Science Foundation of China for support.

Received for review October 27, 2005. Accepted December 27, 2005.

AC051919+